

Report Number 11/45

**A fibrocontractive mechanochemical model of dermal wound
closure incorporating realistic growth factor kinetics**

by

**Kelly E. Murphy, Cameron L. Hall, Philip K. Maini, Scott W.
McCue, and D.L. Sean McElwain**



Oxford Centre for Collaborative Applied Mathematics
Mathematical Institute
24 - 29 St Giles'
Oxford
OX1 3LB
England

A fibrocontractive mechanochemical model of dermal wound closure incorporating realistic growth factor kinetics

Kelly E. Murphy^{a,b,*}, Cameron L. Hall^c, Philip K. Maini^{d,e}, Scott W. McCue^a, D.L. Sean McElwain^{a,b}

^a*Mathematical Sciences, Queensland University of Technology, 2 George St, Brisbane QLD 4000, Australia*

^b*Institute of Health and Biomedical Innovation, Queensland University of Technology, 60 Musk Avenue, Kelvin Grove Urban Village, Kelvin Grove QLD 4059, Australia*

^c*Oxford Centre for Collaborative Applied Mathematics, Mathematical Institute, University of Oxford, 24-29 St Giles', Oxford, OX1 3LB, UK*

^d*Centre for Mathematical Biology, Mathematical Institute, University of Oxford, 24-29 St Giles', Oxford OX1 3LB, UK*

^e*Oxford Centre for Integrative Systems Biology, Department of Biochemistry, University of Oxford, South Parks Road, Oxford, OX1 3QU, UK*

Abstract

Fibroblasts and their activated phenotype, myofibroblasts, are the primary cell types involved in the contraction associated with dermal wound healing. Recent experimental evidence indicates that the transformation from fibroblasts to myofibroblasts involves two distinct processes: the cells are stimulated to change phenotype by the combined actions of transforming growth factor β (TGF β) and mechanical tension. This observation indicates a need for a detailed exploration of the effect of the strong interactions between the mechanical changes and growth factors in dermal wound healing. We review the experimental findings in detail and develop a model of dermal wound healing that incorporates these phenomena. Our model includes the interactions between TGF β and collagenase, providing a more biologically realistic form for the growth factor kinetics than those included in previous

*Corresponding author

Email address: kelly.murphy@qut.edu.au (Kelly E. Murphy)

mechanochemical descriptions. A comparison is made between the model predictions and experimental data on human dermal wound healing and all the essential features are well matched.

Keywords: biomechanics, myofibroblasts, transforming growth factor- β , contraction

1. Introduction

The process of dermal repair is intricate and the resulting scar is inferior to unwounded tissue in several aspects. Aberrant healing may result in pathological scarring that can cause both physical and psychosocial distress to the patient (Herber et al., 2007; Brown et al., 2008, 2010). Understanding and elucidating the mechanisms that elicit normal and regenerative repair is vital to ameliorating the wound healing response.

There are various ways of characterizing the stages of acute healing. A recent description proposed by Enoch et al. (2006), separates wound healing into four overlapping, yet distinct, phases: (1) Haemostasis, which involves arresting blood flow through the establishment of a fibrin clot (Monroe et al., 2010), (2) Inflammation, where neutrophils, macrophages and other leukocytes debride the wound, removing necrotic cells and damaged tissue (Enoch and Leaper, 2007). These cells also release growth factors that attract fibroblasts, the main cell type in dermal repair, to the wound (Shultz et al., 2005). The other stages are (3) Proliferation and (4) Epithelialisation and Remodelling. As the model we describe concerns these final two phases, we now discuss these stages in more detail.

The proliferative phase begins around day 4 post-wounding when fibroblasts are recruited from the surrounding undamaged tissue (Shultz et al., 2005). These cells proliferate and are activated to become myofibroblasts. Both fibroblasts and myofibroblasts function as the primary contractile cells in wound repair, with myofibroblasts exerting stronger cell traction stresses than fibroblasts (Wipff and Hinz, 2009). Together, these cells synthesize proteins such as collagen to replace the fibrin network, and they remodel the resulting collagen lattice (Hinz, 2007). Concurrently, endothelial cells migrate into the wound space, revascularising the wound in a process known as

angiogenesis (Enoch and Leaper, 2007). The proliferating fibroblasts, loose collagen network and neovascularised tissue form a temporary contractile organ known as granulation tissue (Enoch and Leaper, 2007). The contraction of granulation tissue due to the action of fibroblasts and myofibroblasts results in a wound reduction of up to 30% in humans (Desmouliere et al., 1995; Hinz et al., 2001; Farahani and Kloth, 2008) and up to 80% in rats (Farahani and Kloth, 2008). Finally, the onset of reepithelialisation signals the final phase of proliferation.

In the fourth and final stage of wound healing, the outer epidermal layer is restored. Fibroblasts continue to remodel the extracellular matrix, increasing the tensile strength of the wound from approximately 20% to 70% of normal dermal strength after several months of remodelling (Cotran et al., 1999; Singer and Clark, 1999). Finally, a mature scar consisting mainly of collagen develops.

The mathematical literature abounds with investigations into wound repair. Just a sample of the diverse topics considered include angiogenesis (Pettet et al., 1996; Tranqui and Tracqui, 2000; Schugart et al., 2008), the interaction between fibroblast and collagen fibre orientation (Dallon and Sherratt, 1998; Dallon et al., 1999, 2001; McDougall et al., 2006; Cumming et al., 2010), effects due to growth factors (Dale et al., 1997; Vermolen and Javierre, 2010), simple mechanical effects (Tranquillo and Murray, 1992; Tracqui et al., 1995; Murray et al., 1997; Murray, 2003), myofibroblast-enhanced contraction (Olsen et al., 1995, 1996), the interaction between the collagen lattice and extracellular fluid during contraction (Barocas and Tranquillo, 1997), the effects of matrix anisotropy (Cook, 1995), abnormal dermal repair (Vaugh and Sherratt, 2006; Thackham et al., 2008; Xue et al., 2009; Flegg et al., 2010) and models incorporating a combination of wound healing phenomena (Javierre et al., 2009; Hall, 2009; Murphy et al., 2011). However, none of these studies include an explicit description of the mechanical interaction between the cells and their viscoelastic substrate of extracellular matrix (ECM) coupled with a realistic description of the chemical kinetics. We address this issue in the current article.

The first mechanochemical models for dermal wound healing were developed by Murray et al. (1988) and Tranquillo and Murray (1992). The key feature

of these models was the mechanical interaction between the cells and their viscoelastic substrate of extracellular matrix (ECM). The “base” Tranquillo-Murray model comprises three governing equations; two of these stipulate the rate of change of the fibroblast concentration, n , and the ECM density, ρ , respectively, while the third describes a force balance, from which the velocity of the ECM is derived. In one-dimensional Cartesian coordinates, the base non-dimensional model takes the following form:

$$\text{Cells :} \quad \frac{\partial n}{\partial t} + \frac{\partial}{\partial x} \left(n \frac{\partial u}{\partial t} \right) = \frac{\partial^2 n}{\partial x^2} + rn(1 - n); \quad (1)$$

$$\text{ECM :} \quad \frac{\partial \rho}{\partial t} + \frac{\partial}{\partial x} \left(\rho \frac{\partial u}{\partial t} \right) = 0; \quad (2)$$

$$\text{Force Balance :} \quad s\rho u = \frac{\partial}{\partial x} \left(\sigma + \mu \frac{\partial v}{\partial x} + \psi \right); \quad (3)$$

$$\text{Elastic Force :} \quad \sigma = \frac{\partial u}{\partial x}; \quad (4)$$

$$\text{Cell-Traction Force :} \quad \psi = \frac{\tau \rho n}{1 + \gamma n^2}; \quad (5)$$

$$\text{Velocity :} \quad v = \frac{\partial u}{\partial t}; \quad (6)$$

where x is the distance from the wound centre, u is the ECM displacement, μ is the viscosity of the tissue, γ is a parameter quantifying “social loafing” (the amount that a species will stop doing work in the presence of other members of the same species), s is the tethering coefficient of the dermal layer to the subcutaneous tissue, τ is a measure of the fibroblast traction on ECM fibres, and r is the intrinsic growth rate of fibroblasts. The model considers a symmetric wound about $x = 0$, with the wound located on $0 < x < L$, such that $2L$ is the width of the wound. The region $x > L$ corresponds to the surrounding unwounded dermis.

While this seminal model laid the groundwork for much of the subsequent years of research in this area, it neglected some of the essential features of wound healing, such as collagen biosynthesis and heightened collagen density in the wound space. Moreover, this model was unable to describe the significant wound boundary contraction common in dermal repair. While Tranquillo and Murray (1992) did extend their model to incorporate some of these features, the limitations of this formulation, together with the wealth of new experimental data means that a more detailed representation has

become a necessity.

One of the key simplifying assumptions made by Tranquillo and Murray (1992) was that alterations to the ECM do not modify the mechanical properties of the tissue. However, experimental results reveal that this is not the case (Shultz et al., 2005). In the present study, we aim to improve on this model by assuming, like authors such as Ramtani et al. (2002), that tissue elasticity is dependent upon the collagen density.

Olsen and co-workers extended the work of Tranquillo-Murray in a series of papers (Olsen et al., 1995, 1996, 1997, 1998, 1999). Their first advance considered two distinct cellular populations: fibroblasts and myofibroblasts. Inter-conversion between the two phenotypes is assumed, and this is taken to be dependent on the presence of a growth factor (PDGF). Previously, Tranquillo and Murray (1992), in an extension of (1)-(6), assumed a static distribution for the chemical species. To make the description more realistic, Olsen et al. (1995) incorporated a time-dependent representation. Additionally, Olsen and colleagues included collagen synthesis and degradation. Olsen et al. (1995) was able to predict plastic deformation (permanent wound contraction), but only in the absence of collagen kinetics. However, it is now known that matrix turnover is initially rapid, implying that collagen kinetics should not be neglected. Hence, further modelling is required to generate plastic deformation.

The description developed by Tranquillo and Murray (1992) used a purely viscoelastic formulation for the mechanics. Consequently, the system returns to its original state unless a nonhomogeneous spatial distribution of chemical mediator is assumed. With this in mind, Cook (1995) extended Tranquillo and Murray's work by developing a more realistic representation of tissue mechanics that accounts for the structure of a changing, anisotropic ECM. In so doing, Cook was the first to address tissue growth and remodelling and their associated effects upon tissue mechanics. These effects are also considered in Murphy et al. (2011), who also incorporated direct stress coupling between the cells and their mechanical environment.

When cultured under mechanical strain and/or on a stiff substrate, fibroblasts develop actin stress fibres (Grinnell, 2000; Tomasek et al., 2002; Grin-

nell, 2003; Desmouliere et al., 2005). In this state, the cells are termed proto-myofibroblasts, and they exert more cell traction on the ECM than fibroblasts and exhibit upregulated collagen synthesis. Under the action of $\text{TGF}\beta$, proto-myofibroblasts differentiate into myofibroblasts, which are distinguished by the presence of α -smooth muscle actin (α -SMA) (Hinz, 2007; Wells and Discher, 2008; Wipff and Hinz, 2008, 2009; Hinz, 2010). To our knowledge, Javierre et al. (2009) and Murphy et al. (2011) are the only papers to present mathematical models for dermal wound healing that incorporate the stress-dependency of fibroblast to myofibroblast differentiation. However, neither representation considers the proto-myofibroblast stage, instead adopting a combined proto-myofibroblast and myofibroblast population.

The model developed by Javierre et al. (2009) is an extension of the Olsen et al. (1995) model in which PDGF is assumed to be the chemical involved in activating fibroblasts. While PDGF can induce the formation of proto-myofibroblasts, it does not induce transformation to myofibroblasts or expression of α -SMA (Tomasek et al., 2002). Moreover, Javierre et al. (2009) assume that cell traction stress activates fibroblasts, but Hall (2009) found that, for consistency between the mathematical representation and experimental results, the stress component involved in fibroblast activation is the elastic stress and not the cell traction stress. If fibroblast differentiation is assumed to depend on cell traction stress then the greatest activation occurs outside the lesion, i.e. in the unwounded tissue. This is not physiological, as the myofibroblast presence is greatest within the wound space. In contrast, making differentiation depend on the elastic stress would lead to higher rates of conversion within the wound space itself. Moreover, the cell traction stress can be thought of as a convenient representation of what is actually a body force acting on the tissue. By pulling on the tissue, each cell acts as a force dipole; the net effect of these dipoles is a body force determined by the gradient of the cell traction stress. Thus, the elastic stress is the real stress in the ECM, and it is most reasonable to expect that this is the stress that cells will feel and to which they will respond.

Incorporating these observations into a model means that it is impossible to decouple the mechanics from the biology because there is two-way feedback between cellular behaviour and mechanical stress. In the Olsen et al. (1995)

and Tranquillo and Murray (1992) descriptions, passive ECM-mediated advection was the only interaction between the cell and ECM behaviour and the wound mechanics. However, since the velocity was generally small, advection could be neglected without significantly altering the model predictions (Hall, 2009). Consequently, the cellular and ECM components could essentially evolve independent of the mechanics. We argue that this coupling is important in light of recent experimental results and so attempt to resolve this issue by incorporating the stress-dependence in the activation of fibroblasts and myofibroblast proliferation.

The model of Murphy et al. (2011) incorporated some of this feedback between the cells and tissue mechanics. This representation extended the work of Olsen et al. (1995), Cook (1995) and Hall (2009), employing a morphoelastic approach to representing the mechanical behaviour instead of the traditional linear viscoelasticity. This model is more appropriate for the large deformations observed in wound repair, but it neglected to develop a detailed approximation to the chemical kinetics and their associated interactions with cellular and extracellular aspects of repair.

The wound healing model proposed by Dale et al. (1997) does not incorporate tissue mechanics, but it contains the most detailed description of the chemical kinetics of the bioactive species in a dermal wound. Here, we adopt a reduced version of the Dale et al. (1997) model, in spite of the fact that this represents a simplification of the *in-vivo* kinetics. Additionally, we modify the model to incorporate recent experimental results.

When comparing model predictions against experimental data, researchers developing mechanochemical representations of dermal repair typically consider the wound contraction dynamics recorded by McGrath and Simon (1983). However, the wound contraction data obtained by McGrath and Simon (1983) are for rat dermal repair, and mechanochemical modellers are generally seeking to justify a model for human dermal wound healing. Rat and human dermal wounds heal primarily by different mechanisms. While rat wounds heal mainly by contraction, human dermal wounds (while still experiencing contraction) heal primarily as a result of infilling. Thus, we qualitatively compare our predictions against the observations of McGrath and Simon (1983), but seek to ascertain the relevance of our model by com-

paring our predictions against the wound contraction data obtained by Catty (1965) for human dermal repair.

The role of TGF β is now considered to be critical to dermal repair but there are, as yet, no mechanochemical models that consider TGF β as the primary growth factor in dermal repair. Additionally, none include the regulatory effects of collagenase on the collagen density. Here, we incorporate TGF β and collagenase into a simplified representation of chemical kinetics and then couple this with a description of tissue mechanics and cellular dynamics. With regard to cellular interactions, our model includes a novel representation of the fibroblast to myofibroblast activation.

We develop our proposed model in Section 2 below and present the model results in Section 3. Our model predicts early retraction followed by contraction and late retraction. The results are compared with two sets of experimental data on wound closure, that of Catty (1965) for human wounds, and that of McGrath and Simon (1983) for rat dermal repair. We seek only to obtain qualitative agreement with the McGrath and Simon data. Our analysis shows that the model predicts all phases of wound repair (retraction, contraction, permanent contraction and late retraction) for both situations.

2. Mathematical Model

We consider seven dependent variables in our model: fibroblast density (n), myofibroblast density (m), transforming growth factor- β concentration (β), platelet-derived growth factor concentration (P), collagen density (ρ), collagenase density (z), ECM displacement (u) and velocity (v). We assume that the wound is long and thin, and that it is much longer than it is deep. As such, a one-dimensional representation is appropriate.

We assume that a small strain representation is valid and thus the velocity can be approximated by the Eulerian time derivative of displacement:

$$v = \frac{\partial u}{\partial t}. \quad (7)$$

2.1. Force Balance Equation

Following Tranquillo and Murray (1992), we neglect inertial forces and so the momentum conservation equation reduces to a mechanical force balance between the forces related to the physico-chemical ECM properties (consisting of tethering to the underlying fascia, elastic and viscous forces) and the cell-generated traction forces. We assume that the tethering force is proportional to the local collagen concentration and tissue displacement. Together, this gives the following force balance equation:

$$s\rho u = \frac{\partial}{\partial x} \left(\sigma + \mu \frac{\partial v}{\partial x} + \psi \right), \quad (8)$$

where s is the tethering coefficient, μ is the tissue viscosity, and σ and ψ represent the elastic and cell traction forces, respectively.

Since we are considering a linear viscoelastic framework, the elastic force is proportional to the deformation gradient (Skalak et al., 1996). However, we further assume that variations in collagen density will affect the elastic modulus (Ramtani et al., 2002; Ramtani, 2004). Specifically, we will assume that the elastic modulus is directly proportional to the collagen density, with a constant of proportionality, E . Thus, σ takes the form

$$\sigma = E\rho \frac{\partial u}{\partial x}. \quad (9)$$

There are a number of possible expressions for cell traction. Following Tranquillo and Murray (1992), we assume that cell traction forces depend upon the product of the cellular and collagen densities. We also assume that fibroblasts and myofibroblasts contribute differently to cell traction but we do not include any ‘social loafing’ terms. This gives

$$\psi = \lambda\rho(n + \xi m), \quad (10)$$

where λ is a constant and ξ is the myofibroblast tractional stress relative to fibroblast tractional stress. We note that Olsen et al. (1995) assume that myofibroblasts increase the cell traction generated by the fibroblasts, but that myofibroblasts do not work independently to enhance cell traction. However, Tomasek et al. (2002) indicates that myofibroblasts work independently of

fibroblasts to effect contraction. Also we note that other expressions for cell traction could be adopted in which ψ is no longer directly proportional to n , m or ρ (see Tranquillo and Murray, 1992, and Olsen et al., 1995). It is preferable to use the simplest form available for cell traction consistent with experimental observations, and so we adopt the above expression.

2.2. Fibroblasts

We assume that the fibroblasts exhibit random motility (modelled by diffusion), PDGF-mediated chemotaxis and experience ECM-mediated advection. TGF β stimulates fibroblast proliferation which, in the absence of other factors, is assumed to be logistic. Fibroblast to myofibroblast transformation requires tension (represented by positive elastic stress) and the presence of active TGF β . Hence, we obtain

$$\begin{aligned} \frac{\partial n}{\partial t} + \frac{\partial}{\partial x} (nv) = & \frac{\partial}{\partial x} \left[D_n \frac{\partial n}{\partial x} - \frac{\chi n}{(a_\chi + P)^2} \frac{\partial P}{\partial x} \right] \\ & + (1 + a_{n\beta}\beta) n (r - \theta_{nn}n) - \alpha \sigma^+ \beta n, \end{aligned} \quad (11)$$

where D_n is the fibroblast random motility coefficient, χ is the chemotactic coefficient, a_χ represents the half-maximal response, α is the fibroblast differentiation rate, σ^+ represents the positive elastic stress, $a_{n\beta}$ represents the upregulation of fibroblast proliferation in the presence of TGF β , r is the intrinsic fibroblast proliferation rate and θ_{nn} represents the reduction in proliferation due to crowding.

Since there is insufficient experimental evidence to suggest otherwise, we assume that myofibroblasts do not transform back to fibroblasts, but instead undergo apoptosis (Moulin et al., 2004; Hinz, 2007; Farahani and Kloth, 2008). However, we note that Olsen et al. (1995) include the reversion of myofibroblasts to fibroblasts. Moreover, we do not include a proto-myofibroblast population, and instead consider a combined proto-myofibroblast and myofibroblast population, which we simply refer to as myofibroblasts.

2.3. Myofibroblasts

Without evidence that myofibroblasts are actively motile, we assume that their transport is due only to ECM-mediated advection. As long as the granulation tissue is under stress, myofibroblasts will proliferate (Grinnell, 1994; Hinz, 2007). Hence, we follow Hall (2009) and assume that myofibroblasts only proliferate under stress and that this growth is bounded. Finally, myofibroblasts undergo natural cell death. Together, these assumptions give

$$\frac{\partial m}{\partial t} + \frac{\partial}{\partial x}(mv) = m(a_{m\sigma}\sigma^+(1 + a_{m\beta}\beta) - \theta_m - \theta_{mm}m) + \alpha\sigma^+\beta n, \quad (12)$$

where $a_{m\beta}$ represents the upregulation in myofibroblast proliferation under the action of TGF β , $a_{m\sigma}$ is the intrinsic myofibroblast proliferation rate under tension, θ_m is the natural cell death rate and θ_{mm} represents the decrease in proliferation due to crowding.

2.4. TGF β

TGF β diffuses and is passively advected by the ECM. This growth factor is produced by both fibroblasts and myofibroblasts (Hinz, 2007; Wipff et al., 2007), with production inhibited by the presence of TGF β (Dale et al., 1996). We recognise that TGF β is synthesized by cells in a latent form, which is then activated by one of two mechanisms. These are the activation by myofibroblasts from large latent complex stores attached to the ECM (Wipff et al., 2007; Wells and Discher, 2008) and the cleavage of circulating latent TGF β by collagenases (Dale et al., 1996). For simplicity, we consider a combined latent and active TGF β species. TGF β also undergoes natural decay. Incorporating all of these effects into a model, we obtain:

$$\frac{\partial \beta}{\partial t} + \frac{\partial}{\partial x}(\beta v) = D_\beta \frac{\partial^2 \beta}{\partial x^2} + \frac{a_\beta \beta (n + \pi m)}{1 + b_\beta \beta} + a_{\beta m} m \rho + a_{\beta z} z \beta - \delta_\beta \beta, \quad (13)$$

where D_β is the TGF β diffusivity, a_β characterizes the production rate of TGF β by fibroblasts, π is the ratio of myofibroblast to fibroblast production of TGF β , $a_{\beta m}$ is the activation rate of TGF β from matrix stores, $a_{\beta z}$ is the activation rate of latent TGF β by collagenases and δ_β is the decay rate of TGF β . We adopt a saturation form for the production of TGF β , with b_β related to the half-maximal rate of production.

2.5. PDGF

Macrophages and other cells produce PDGF, which we assume occurs at a constant rate, a_P . PDGF also experiences natural decay and fibroblast-mediated depletion through endocytosis. Finally, PDGF diffuses and is advected by the ECM. Thus,

$$\frac{\partial P}{\partial t} + \frac{\partial}{\partial x}(Pv) = D_P \frac{\partial^2 P}{\partial x^2} + a_P - \delta_P P - \delta_{Pn} nP, \quad (14)$$

where D_P is the PDGF diffusivity, δ_P represents natural decay and δ_{nP} fibroblast-mediated PDGF depletion.

2.6. Collagen

Collagen undergoes ECM-mediated advection and is synthesized by both cell types, with production upregulated by the presence of TGF β . Additionally, collagen is degraded by the action of collagenases. Thus, we obtain

$$\frac{\partial \rho}{\partial t} + \frac{\partial}{\partial x}(\rho v) = k(n + \eta m)(1 + a_{\rho\beta}\beta) - \delta_{\rho}\rho z, \quad (15)$$

where k characterizes the production rate of collagen by fibroblasts, η is the ratio of myofibroblast to fibroblast collagen production, $a_{\rho\beta}$ is a measure of the increase in synthesis due to the presence of TGF β and δ_{ρ} is the degradation rate. Note that we refer to collagen and ECM interchangeably throughout the rest of this paper, since dermal ECM consists mainly of collagen.

2.7. Collagenase

While several species of collagenase are involved in the wound healing process, we consider here a general representation of these enzymes. Since collagenase binds to the local ECM, we assume that diffusion is negligible and thus collagenase transport is only by ECM-mediated advection (Dale et al., 1997). Both fibroblasts and myofibroblasts secrete collagenase in the presence of collagen, with production of collagenase inhibited by the presence of active TGF β (Wipff and Hinz, 2009). Furthermore, collagenase undergoes

natural decay. Putting this together, we have

$$\frac{\partial z}{\partial t} + \frac{\partial}{\partial x}(zv) = \frac{a_z \rho(n + \zeta m)}{1 + b_z \beta} - \delta_z z, \quad (16)$$

where a_z characterizes the production rate of collagenase by cells in the presence of collagen, ζ is the rate of myofibroblast collagenase synthesis relative to fibroblast collagenase synthesis, b_z measures the inhibition of collagenase synthesis due to the presence of TGF β , and δ_z is the collagenase decay rate.

We note that collagenase is secreted by cells in a latent form that is activated through proteolytic cleavage. Dale et al. (1997) incorporate this feature into their model. However, for simplicity, we have chosen to combine the latent and active forms of collagenase as a single species. We also note that collagenases are a subset of the matrix metalloproteinases (MMPs) and that the collagenase in this model could be identified with MMP-1. Both Chakraborti et al. (2003) and Jenkins (2008) provide extensive reviews of MMPs in ECM.

2.8. Initial/Boundary Conditions and Non-Dimensionalization

The initial conditions of our model refer to the state of the wound at the onset of the proliferative phase. At this stage, we take the wound to occupy $-L < x < L$, so that L represents the wound boundary. We assume:

1. Symmetry about $x = 0$, and so we can restrict ourselves to considering the domain where x is positive;
2. $x > L$ represents unwounded tissue;
3. The characteristic time scale of the model, T , is one day;
4. There are no fibroblasts within the wound space and they are at unwounded levels outside;
5. The initial myofibroblast density is zero everywhere;
6. Due to growth factor release in the inflammatory stage, TGF β is present inside the wound space, but not outside;
7. Within the wound, PDGF is initially at its steady state value in the case of no fibroblasts, while outside the lesion PDGF takes its

steady state value appropriate for the situation in which fibroblasts are present;

8. There is a small amount of collagen in the wound space initially, while unwounded levels prevail outside; and
9. Collagenase is only produced in the presence of collagen, and thus that there is no collagenase in the wound initially and that it is at unwounded levels outside.

To avoid discontinuities which can give rise to numerical instabilities when solving the PDE system we approximate these piecewise conditions using *tanh* functions (see Appendix B for details).

Immediately following injury, there is an almost instantaneous retraction of the wound boundary (see for example Billingham and Medawar, 1955, Catty, 1965). Indeed, the unwounded dermis surrounding the wound has an elastic tension that tends to draw the wound edges apart (Watts, 1960; Kennedy and Cliff, 1979). Therefore, the initial displacement is not zero throughout the domain, but is rather found by demanding the force balance expression (8) hold. Since this initial retraction is driven by elastic tension, we neglect viscosity when determining the initial displacement.

The symmetry around $x = 0$ implies zero flux conditions for all species other than displacement and velocity, which must necessarily be zero at the wound centre. For numerical purposes all species are assumed to take on their unwounded values at the right-hand boundary (far away from the wound site),

$$\begin{aligned} n(x_{RH}, t) &= n_U, & m(x_{RH}, t) &= 0, & \beta(x_{RH}, t) &= \beta_U, & P(x_{RH}, t) &= P_U, \\ \rho(x_{RH}, t) &= \rho_U, & z(x_{RH}, t) &= z_U, & u(x_{RH}, t) &= 0, \end{aligned}$$

where x_{RH} is the position of the right hand boundary and $x_{RH} \gg L$, and n_U , β_U , P_U , ρ_U and z_U represent the unwounded densities of fibroblasts, TGF β , collagen and collagenases, respectively.

The system was non-dimensionalized (see Appendix A), discretised using finite difference approximations in space and solved numerically using MATLAB's inbuilt routine, *ode45*. We consider a grid size of 401 and a compu-

tational domain of 10 semi-wound lengths; this ensures that the right hand boundary is far enough from the wound site so as not to affect the solution within the wound. Grid independent results are obtained providing the grid size exceeds 301 nodes. Advective terms are determined by solving the tri-diagonal system obtained by discretising the force balance expression, (8), with displacement found by subsequently using (7).

2.9. Parameter Values

Almost all parameter values have been estimated from experimental results or taken from previous models of dermal repair. Table 1 contains the dimensional values of the parameters together with the source of the data; if a given parameter has been estimated in this work, this is indicated by TW. The sensitivity analysis shows our model to be quite robust to significant variations in a number of parameter values. For a full discussion on parameter estimation see Appendix C.

3. Results and Discussion

Figures 1, 3 and 4 show the results obtained from the numerical solution of the system of governing equations and we now discuss these in detail.

3.1. Fibroblasts

Initially, there are no fibroblasts inside the wound space and they are at unwounded levels outside. While fibroblasts are recruited from the surrounding dermis, proliferation is the primary mode by which the fibroblast population within the wound space is restored. There is significant conversion of fibroblasts to myofibroblasts over the first fortnight of repair, which accounts for the unusual shape of the fibroblast distribution. Indeed, the mechanical stimulation of fibroblast activation impedes the restoration of the fibroblast density within the wound space through modulation to myofibroblasts. Nonetheless, by day 30 the fibroblast density across the domain has essentially been restored to undamaged tissue values. We note that varying the chemotactic coefficient has little impact on the model predictions.

Parameter	Range	Reference
D_n , Fibroblast random motility	$D_n \approx O(10^{-3})\text{cm}^2/\text{day}$	Sillman et al. (2003)
χ , Chemotaxis	$\chi = 4.78 \times 10^{-3}\text{ng}/\text{cm}\cdot\text{day}$	Menon et al. (2011)
a_χ , Half-maximal response	$a_\chi = 47.8\text{ng}/\text{cm}^3$	Menon et al. (2011)
r , Fibroblast proliferation	$0.832 < r < 0.924/\text{day}$	Ghosh et al. (2007)
$a_{n\beta}$, Enhancement of fibroblast proliferation by $\text{TGF}\beta$	$2/\beta_0$	Strutz et al. (2001)
θ_{nn} , 1/Fibroblast carry capacity	10^{-6}cells	Vande Berg et al. (1989)
α , Fibroblast activation to myofibroblasts	$r \approx 0.0108/\text{day}\cdot(\text{ng}/\text{mL})$	Desmouliere et al. (1993)
$a_{m\sigma}$, Myofibroblast proliferation	$a_{m\sigma} = 0.25r$	TW
$a_{m\beta}$, Enhancement of myofibroblast proliferation by $\text{TGF}\beta$	$a_{m\beta} = a_{n\beta}$	Olsen et al. (1995)
θ_m , Myofibroblast apoptosis	$\theta_m \approx 0.9/\text{day}$	Olsen et al. (1995)
θ_{mm} , 1/Myofibroblast carrying capacity	$\theta_{mm} = 2\theta_{nn}$	Masur et al. (1996)
D_β , $\text{TGF}\beta$ diffusivity	$0.0254\text{cm}^2/\text{day}$	TW
a_β , $\text{TGF}\beta$ synthesis by fibroblasts	$0.125 \times 10^{-6}\text{ng}/\text{cell}\cdot\text{day}$	TW
π , $\text{TGF}\beta$ synthesis by myofibroblasts relative to fibroblasts	2	TW
b_β , Inhibition of $\text{TGF}\beta$ synthesis	$0.0013\text{mL}/\text{ng}$	Dale (1995)
$a_{\beta m}$, $\text{TGF}\beta$ activation by myofibroblasts	$4.35 \times 10^{-9}\text{mL}\cdot\text{day}/\text{cell}$	TW
$a_{\beta z}$, $\text{TGF}\beta$ activation by proteolytic cleavage	$0.00144\text{ng}/\text{cell}$	TW
δ_β , $\text{TGF}\beta$ decay	$b \approx 0.354/\text{day}$	Yang et al. (1999)
D_P , PDGF diffusion coefficient	$D_P = 2.4 \times 10^{-3}\text{cm}^2/\text{day}$	Haugh (2006)
a_P , PDGF production	$a_P = 115\text{ng}/\text{cm}^3\cdot\text{day}$	Menon et al. (2011), TW
δ_P , PDGF degradation	$\delta_P = 2.4/\text{day}$	Haugh (2006)
δ_{Pn} , fibroblast-mediated PDGF depletion	$\delta_{Pn} = 48 \times 10^{-6}/\text{cell}\cdot\text{day}$	Haugh (2006)
k , Collagen production	$1.75\text{pg}/\text{cell}\cdot\text{day}$	Menon et al. (2011), TW
η , Relative collagen production by myofibroblasts	2	Bahar et al. (2004)
$a_{\rho\beta}$, Enhancing of collagen production by $\text{TGF}\beta$	$2/\beta_0$	Moulin et al. (1998), Olsen et al. (1995)
δ_ρ , Collagen degradation	$0.3k$	Eickelberg et al. (1999)
a_z , Collagenase production	$4.73 \times 10^{-9}\text{mL}^2/\text{ng}^2\cdot\text{day}^{-1}$	Aumailley et al. (1982)
ζ , Relative collagenase production by myofibroblasts	2	TW
b_z , Inhibition of collagenase production by $\text{TGF}\beta$	$3/\beta_0$	Overall et al. (1991)
δ_z , Collagenase decay	$0.3616/\text{day}$	Overall et al. (1991)
s , Tethering coefficient	1	Olsen et al. (1995)
μ , Viscosity	$O(10)$	Olsen et al. (1995)
Y , Elastic modulus	$10 < Y < 300\text{N}$	Silver et al. (2001), Genzer and Groenewold (2006)
τ , Fibroblast cell traction	$1 < \tau < 3\mu\text{N}/\text{cell}$	Wrobel et al. (2002), Fray et al. (1998)
ζ , Ratio of myofibroblast to fibroblast cell traction	$\zeta \approx 2$	Wrobel et al. (2002)
β_0 , Initial $\text{TGF}\beta$ concentration	$275\text{ng}/\text{mL}$	Yang et al. (1999)

Table 1: Table of parameters, which unless otherwise specified, are used for all simulations. TW refers to parameters that were estimated during this work.

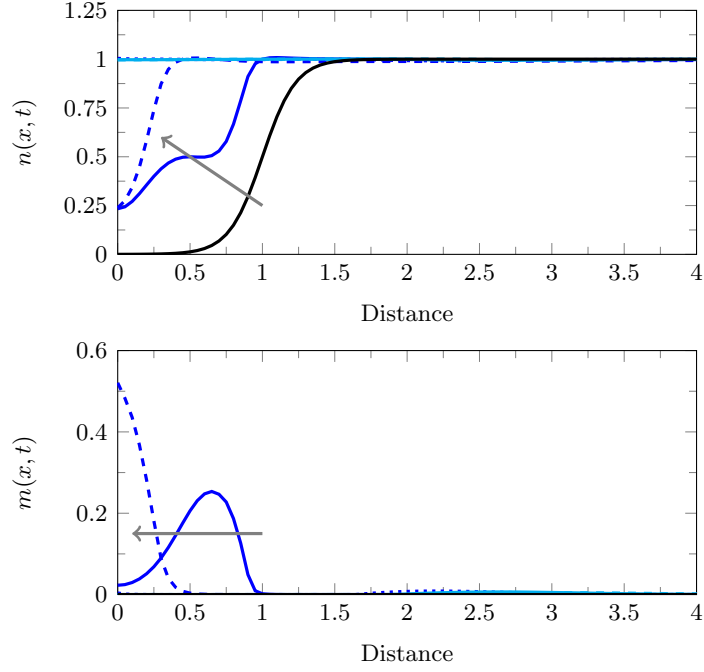


Figure 1: Model predictions for the fibroblast and myofibroblast densities, and the TGF β concentration. Black solid curves represent the initial condition of each species. Dashed then dotted curves follow alternately, with an incremental time step of 6 days out to 30 days. The computational domain is ten semi-wound lengths, so that $0 < x < 10$. In order to show behaviour in the wound more clearly, only the domain $0 < x < 4$ is shown. Arrows indicate the direction of increasing time. Parameter values are given by $D_n = 0.001$, $\chi = 0.0001$, $a_\chi = 1$, $\alpha = 3$, $a_{n\beta} = 2$, $r = 0.832$, $a_{m\beta} = 2$, $a_{m\sigma} = 0.21$, $\theta_m = 0.9$, $\theta_{mm} = 0.41$, $D_\beta = 0.025$, $a_\beta = 0.1$, $\eta = 2$, $b_b = 0.3$, $a_{\beta z} = 0.25$, $a_{\beta m} = 0.21$, $\delta_\beta = 0.35$, $D_P = 0.0024$, $a_P = 2.4$, $\delta_P = 2.4$, $\delta_{Pn} = 40$, $\kappa = 0.1$, $\pi = 2$, $a_{\rho\beta} = 2$, $\omega = 0.2$, $\zeta = 2$, $b_z = 5$, $s = 1$, $\mu = 20$, $E = 10$, $\lambda = 2.2$, $\xi = 2$.

3.2. Myofibroblasts

Initially, there are no myofibroblasts in the system. Fibroblasts are activated to become myofibroblasts under the action of elastic stress and $\text{TGF}\beta$, and, for this parameter set, this conversion is found to be the primary source of myofibroblasts. Differentiation of fibroblasts generates a population of myofibroblasts within the wound domain, which proliferate and generate stress. Thus, myofibroblasts contribute to both wound contraction and further fibroblast activation. Fibroblasts continue to transform to myofibroblasts, with the greatest density of myofibroblasts occurring where the elastic stress is highest. There is a small level of myofibroblast activation predicted outside the wound due to small elastic stresses and the presence of a small concentration of $\text{TGF}\beta$ there. At long time, both the elastic stress and $\text{TGF}\beta$ tend to zero, and so the myofibroblast density tends to zero also (results not shown).

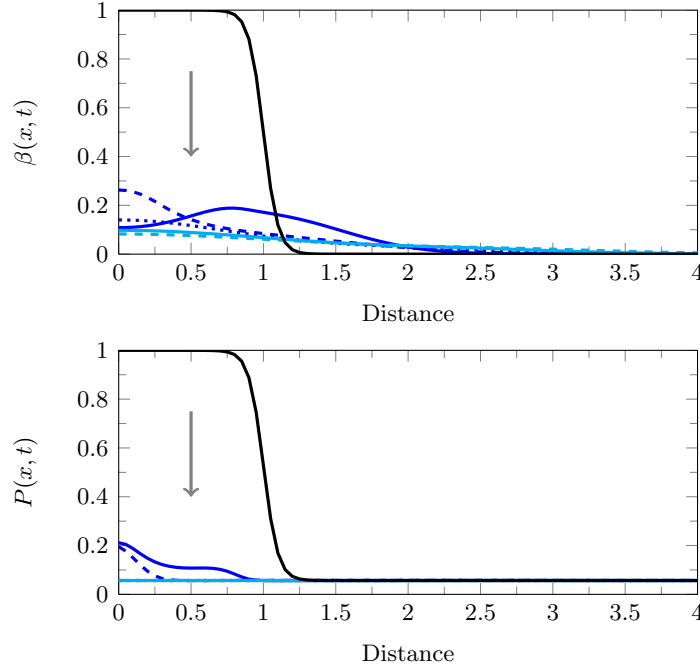


Figure 2: Model predictions for the $\text{TGF}\beta$ and PDGF concentration. Black solid curves represent the initial condition of each species. Dashed then dotted curves follow alternately, with an incremental time step of 6 days. Arrows indicate the direction of increasing time. Parameter values are the same as Figure 1.

3.3. Transforming Growth Factor β

TGF β appears early in the wound healing process as a result of the inflammatory cascade. Since there is no active TGF β in unwounded dermis, the TGF β concentration is initially zero outside the wound space (see Figure 1). The concentration of TGF β within the wound is gradually depleted through natural decay. However, both fibroblasts and myofibroblasts produce TGF β and it can be activated through cleavage by collagenase and from latent stores in the matrix by myofibroblasts. As a result, the decay of TGF β is quickly stemmed, which explains why it is still present at day 30, and why there is an increase in TGF β around the wound boundary for early times. At later times, the TGF β concentration tends to zero throughout. We note that our expression for myofibroblast activation of TGF β from local matrix stores assumes that fibroblasts and myofibroblasts bind more TGF β to the ECM than can be activated when the myofibroblasts contract the collagen fibers. Hence it is assumed that there is always a supply of TGF β attached to the matrix available for activation, which may or may not be accurate.

3.4. PDGF

Platelets release huge quantities of PDGF early in repair, yielding the significantly higher concentration of PDGF inside the wound initially. As fibroblasts repopulate the wound space, fibroblast-mediated depletion of PDGF occurs until the PDGF concentration attains unwounded levels within the lesion.

3.5. Collagen

Initially we assume that there is a low density of collagen within the wound while the density is at unwounded levels outside. Synthesis of collagen by both fibroblasts and myofibroblasts is the primary source of collagen. The wound is largely healed as a result of infilling, consistent with experiments on human dermal repair (Catty, 1965). Collagen production by cells is upregulated by the presence of TGF β . This fact, combined with the near-unwounded levels of fibroblasts and the high density of myofibroblasts, gives

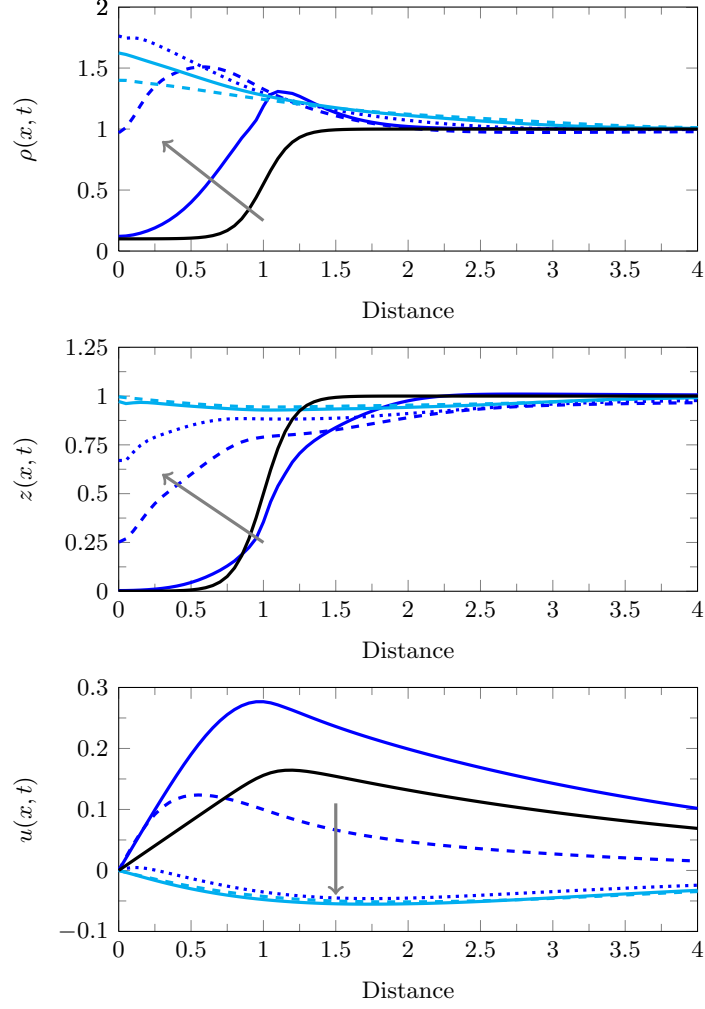


Figure 3: Model predictions for the collagen density, collagenase concentration and collagen displacement. Black solid curves represent the initial condition of each species. Dashed then dotted curves follow alternately, with an incremental time step of 6 days. Arrows indicate the direction of increasing time. Parameter values are the same as Figure 1. We note that the computational domain is ten semi-wound lengths, such that $0 < x < 10$, and that the displacement, u , does tend to zero at the right hand boundary.

rise to excess collagen within the wound space; as we see, the collagen profile is very similar to the $\text{TGF}\beta$ profile. While not shown in Figure 3, remodelling by the fibroblasts at later times ensures that the collagen density ultimately tends to unwounded levels throughout the domain.

3.6. Collagenase

It is assumed that there is no collagenase within the wound initially, but that the collagenase is at unwounded levels outside. The collagenase concentration inside the lesion decreases at early times, which can be attributed to the large early retraction. As the cells synthesize collagenase, the production is inhibited by the presence of $\text{TGF}\beta$, and collagenase secretion is lowest at the wound centre where the $\text{TGF}\beta$ concentration is highest. Collagenase levels eventually tend to unwounded levels. Since collagenase is non-zero at steady state, this implies that there is a balance reached between collagenase production and degradation at steady state. Furthermore, this suggests that there is continuous turnover of ECM in unwounded tissue, which is consistent with clinical observations (Roberts et al., 1990).

3.7. Wound Boundary

The current position of the wound boundary can be obtained by finding the point x , where the dimensionless displacement satisfies

$$x_{wb} = 1 + u(x_{wb}, t). \quad (17)$$

Thus, x_{wb} represents the material point that was located at $x = 1$ when $t = 0$. The movement of the wound boundary is represented by the black curves in Figure 4.

Figures 4a and 4b show the comparison between our predicted curve and the data obtained by Catty (1965) for human wounds. Our model predicts the large initial retraction, and slow contraction of the wound, agreeing well with the data. However, our model does not predict an initial scaled wound boundary position of unity. This is because our model begins after the almost-instantaneous retraction that occurs following injury. In addition, whilst our model does predict a small late retraction, we did not observe

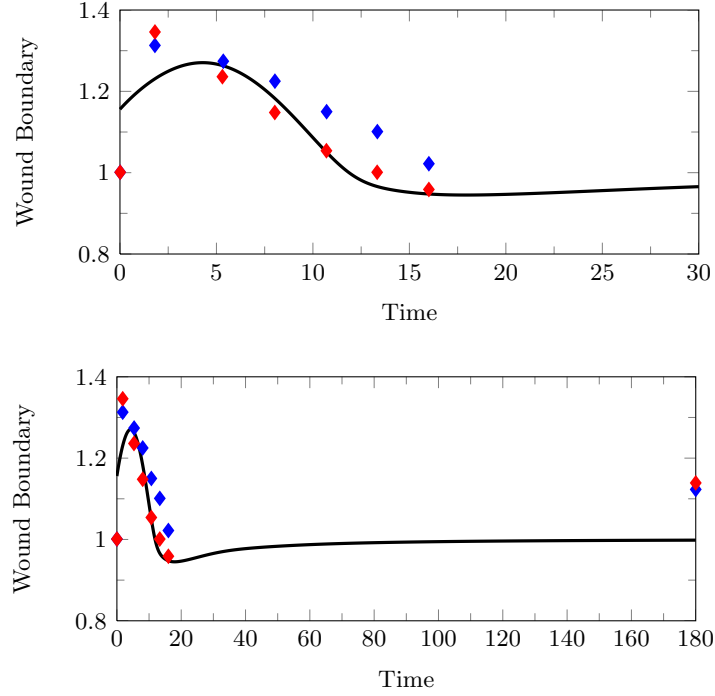


Figure 4: The wound boundary prediction from our model is the black curve. Two series of data for human wound closure were obtained from Catty (1965). Series A and B correspond to the red and blue points respectively. The daily collection of wound boundary data ceased at day 16 post wounding. One further measurement was made at 6 months. Parameter values are the same as Figure 1.

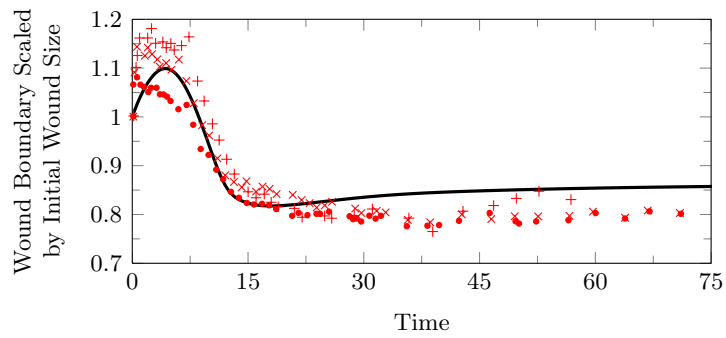


Figure 5: The wound boundary prediction from our model is the black curve, and has been scaled respective to the initial wound size. Data showing the contractile phases of wound closure were obtained from McGrath and Simon (1983) for circular (●), small square (+) and large square (×) wounds respectively. Parameter values are the same as Figure 1.

the large late retraction seen by Catty. Apart from these few data points however, good agreement is seen between the data of Catty (1965) and our prediction curves. This is especially true when examining the early expansion and contraction measurements.

Table 2 gives the values for expansion (or retraction), contraction and late retraction observed by both Catty and colleagues and our simulation curve. We note that our model did not predict the maximum retraction to occur at day 16, but rather at day 18. Hence, we give two “healed” estimates: the predicted day 16 result and the value obtained at the maximum contraction (day 18). However, the day 16 and 18 predictions differ very little and both indicate that the majority of contraction occurs during the first three weeks of wound repair. These predictions are very similar to those obtained by Catty (1965), aside from the post 6-months column. This again confirms that for the proliferative stage of wound repair that we are modelling, good agreement is seen between the model predictions and the data.

Series	Actual Area (sq. cm.)	Pre- Excision	Post- Excision	Healed		Six Months
A	1.01	1.000	1.316	1.041		1.123
B	1.07	1.000	1.343	0.960		1.139
Model	-	1.000	1.279	Day 16	Max	0.998
				0.942	0.947	

Table 2: Data reproduced from Catty (1965) together with the corresponding predictions from our model. The healed model value at day 16 corresponds to the point when Catty terminated the daily measurements, while ‘max’ represents the predicted maximum contraction from the model at day 18. Series A contained 11 patients, while Series B had 9 patients. Pre-excision refers to the area to be removed from the patient, actual area indicates the area of tissue actually excised, post-excision is the area of the wound after the retraction or expansion of the wound following removal of the tissue, healed refers to the day 16 values while six months values refer to the amount of retraction observed six months following wounding, as measured by Catty and predicted by the model.

We note from Table 2 that the expansion and healed values are comparable. With regard to the amount of late retraction predicted by our model, we were not able to obtain the large retraction observed by Catty (1965). However, the purpose of our model was to simulate the proliferative phase of wound

repair, and so it is really only appropriate for the first 30 days of wound repair; during this time, the model compares well with the experimental data.

In Figure 5 we consider the same simulation curve, but in this case we compare our prediction of wound closure qualitatively against the McGrath and Simon (1983) data for rat dermal repair. Rat wounds exhibit far greater contraction than do human dermal injuries. Consequently, we scale the data from McGrath and Simon (1983) using

$$y_{\text{scaled}} = \frac{5}{7} + \frac{2}{7}y_{\text{data}}, \quad (18)$$

so that comparable contraction is observed in both the data and the model predictions. This scaling is sensible as human wounds heal with almost a third the contraction observed in rat dermal repair.

We see from the figure that the initial retraction, contraction, permanent contraction and late retraction observed in the data of McGrath and Simon (1983) are all predicted by our model. Hence, not only does our model correctly predict the closure of human dermal wounds, it reproduces all the phenomena found in murine dermal wound closure. Therefore, we believe this model represents a reasonable description of the closure of dermal wounds.

Our model predicts the large retraction and subsequent contraction seen during the first month of human dermal repair, a phenomenon not considered in previous mechanochemical representations of wound healing. The large retraction is due to the absence of fibroblasts and collagen within the wound space, and the contraction occurs following infilling as the fibroblasts and myofibroblasts contract the newly formed collagen matrix.

Previous researchers have not addressed the manner in which $\text{TGF}\beta$ and tissue mechanics inform the activation of fibroblasts to myofibroblasts. Our model predicts that it is the elimination of $\text{TGF}\beta$ from the system, together with the reduction in local tension that reduces the presence of myofibroblasts towards the end of the proliferative phase.

Our model investigates the complex interactions between cells, $\text{TGF}\beta$ and

collagenase in the regulation of collagen expression. During the period when the $\text{TGF}\beta$ concentration is high, we found that collagen expression is heightened within the wound space. This can be attributed to both the presence of myofibroblasts and to the increased production of collagen by both fibroblasts and myofibroblasts in the presence of $\text{TGF}\beta$. The myofibroblast density and $\text{TGF}\beta$ concentration tend to zero, but remodelling of the collagen network by fibroblasts and collagenase continues, so that the collagen density approaches healed levels across the wound space.

We now discuss possible extensions of this model. Wound geometry and depth are known to play a role in the rapidity of repair (Billingham and Russell, 1956; McGrath and Simon, 1983). Thus, one could extend the current model to two dimensions to investigate the impact of these phenomena on healing. Another possibility would be to analyse how repair is affected by wound debridement, in which the granulation tissue and other constituents are removed. Alternatively, it would be possible to examine the effect of addition or removal of $\text{TGF}\beta$. Indeed, Ferguson and O’Kane (2004) found that addition of different isoforms of $\text{TGF}\beta$ can improve or exacerbate repair. Therefore, one may wish to distinguish between the $\text{TGF}\beta$ isoforms instead of considering a general $\text{TGF}\beta$ distribution.

As our model includes $\text{TGF}\beta$, collagenase and collagen, it can be used to investigate wound healing pathologies, such as keloid development, where the interactions between these three species are significant. In future work, we will examine the formation of keloids using an extension of this model.

Finally, another key process involved during the proliferative phase is angiogenesis. We intend to couple this system together with a representation of angiogenesis to examine the combined effect of inflammation, fibroplasia and angiogenesis in wound closure.

Acknowledgements

This research is primarily supported under the Australian Research Council’s Discovery Projects funding scheme (project number DP0878011), the Institute of Health and Biomedical Innovation at Queensland University of Technology and by the Centre for Mathematical Biology, Mathematical

Institute at the University of Oxford. PKM was partially supported by a Queensland University of Technology Adjunct Professorship and a Royal Society Wolfson Research Merit Award. This publication was based on work supported in part by Award No. KUK-C1-013-04, made by King Abdullah University of Science and Technology (KAUST).

References

- M. Aumailley, T. Krieg, G. Razaka, P.K. Müller, and H. Bricaud. Influence of cell density on collagen biosynthesis in fibroblast cultures. *Biochemical Journal*, 206: 505–510, 1982.
- M.A. Bahar, B. Bauer, E.E. Tredget, and A. Ghahary. Dermal fibroblasts from different layers of human skin are heterogeneous in expression of collagenase and types I and III procollagen mRNA. *Wound Repair and Regeneration*, 12:175–182, 2004.
- V.H. Barocas and R.T. Tranquillo. An anisotropic biphasic theory of tissue-equivalent mechanics: the interplay among cell traction, fibrillar network deformation, fibril alignment, and cell contact guidance. *Journal of Biomechanical Engineering*, 119:137–145, 1997.
- R.E. Billingham and P.B. Medawar. Contracture and intussusceptive growth in the healing of extensive wounds in mammalian skin. *Journal of Anatomy*, 89: 114–123, 1955.
- R.E. Billingham and P.S. Russell. Studies on wound healing, with special reference to the phenomenon of contracture in experimental wounds in rabbits’ skin. *Annals of Surgery*, 144:961–981, 1956.
- B.C. Brown, S.P. McKenna, K. Siddhi, D.A. McGrouther, and A. Bayat. The hidden cost of skin scars: quality of life after skin scarring. *Journal of Plastic, Reconstructive and Aesthetic Surgery*, 61:1049–1058, 2008.
- B.C. Brown, T.P. Moss, D.A. McGrouther, and A. Bayat. Skin scar preconceptions must be challenged: Importance of self-perception in skin scarring. *Journal of Plastic, Reconstructive and Aesthetic Surgery*, 63:1022–1029, 2010.
- R.H.C. Catty. Healing and contraction of experimental full-thickness wounds in the human. *British Journal of Surgery*, 52:542–548, 1965.
- Inc. Cell Signaling Technology. Growth factors & cytokines. Published online at Cell Signaling Technology, URL: <http://www.cellsignal.com/products/8916.html>, 2010.

- S. Chakraborti, M. Mandal, S. Das and A. Mandal, and T. Chakraborti. Regulation of matrix metalloproteinases: An overview. *Molecular and Cellular Biochemistry*, 253:269–285, 2003.
- J. Cook. *A mathematical model for dermal wound healing: wound contraction and scar formation*. PhD thesis, University of Washington, 1995.
- R.S. Cotran, V. Kumar, and T. Collins. *Robbins Pathologic Basis of Diseases*. W.B. Saunders Company, 6 edition, 1999.
- B.D. Cumming, D.L.S. McElwain, and Z. Upton. A mathematical model of wound healing and subsequent scarring. *Journal of The Royal Society Interface*, 7:19, 2010.
- P. Dale. *Time heals all wounds? Mathematical models of Epithelial and Dermal Wound Healing*. PhD thesis, University of Oxford, 1995.
- P.D. Dale, J.A. Sherratt, and P.K. Maini. A mathematical model for collagen fibre formation during foetal and adult dermal wound healing. *Proceedings: Biological Sciences*, 263:653–660, 1996.
- P.D. Dale, J.A. Sherratt, and P.K. Maini. Role of fibroblast migration in collagen fiber formation during fetal and adult dermal wound healing. *Bulletin of Mathematical Biology*, 59:1077–1100, 1997.
- J.C. Dallon and J.A. Sherratt. A mathematical model for fibroblast and collagen orientation. *Bulletin of Mathematical Biology*, 60:101–129, 1998.
- J.C. Dallon, J.A. Sherratt, and P.K. Maini. Mathematical modelling of extracellular matrix dynamics using discrete cells: Fiber orientation and tissue regeneration. *Journal of Theoretical Biology*, 199:449–471, 1999.
- J.C. Dallon, J.A. Sherratt, and P.K. Maini. Modeling the effects of transforming growth factor- β on extracellular matrix alignment in dermal wound repair. *Wound Repair and Regeneration*, 9:278–286, 2001.
- A. Desmouliere, A. Geinoz, F. Gabbiani, and G. Gabbiani. Transforming growth factor- β 1 induces α -smooth muscle actin expression in granulation tissue myofibroblasts and in quiescent and growing cultured fibroblasts. *The Journal of Cell Biology*, 122:103–111, 1993.
- A. Desmouliere, M. Redard, I. Darby, and G. Gabbiani. Apoptosis mediates the decrease in cellularity during the transition between granulation tissue and scar. *American Journal of Pathology*, 146:56–66, 1995.

- A. Desmouliere, C. Chaponnier, and G. Gabbiani. Tissue repair, contraction, and the myofibroblast. *Wound Repair and Regeneration*, 13:7–12, 2005.
- O. Eickelberg, E. Kohler, F. Reichenberger, S. Bertschin, T. Woodtli, P. Erne, A.P. Perruchoud, and M. Roth. Extracellular matrix deposition by primary human lung fibroblasts in response to TGF- β 1 and TGF- β 3. *American Journal of Physiology - Lung Cellular and Molecular Physiology*, 276:814–824, 1999.
- S. Enoch and D.J. Leaper. Basic science of wound healing. *Surgery*, 26:31–37, 2007.
- S. Enoch, J.E. Grey, and K.G. Harding. ABC of wound healing: Recent advances and emerging treatments. *British Medical Journal*, 332:962–965, 2006.
- R.M. Farahani and L.C. Kloth. The hypothesis of ‘biophysical matrix contraction’: wound contraction revisited. *International Wound Journal*, 5:477–482, 2008.
- M.W.J. Ferguson and S. O’Kane. Scar-free healing: from embryonic mechanisms to adult therapeutic intervention. *Philosophical Transactions of the Royal Society of London B*, 359:839–850, 2004.
- J.A. Flegg, H.M. Byrne, and D.L.S. McElwain. Mathematical model of hyperbaric oxygen therapy applied to chronic diabetic wounds. *Bulletin of Mathematical Biology*, 72:1867–1891, 2010.
- T.R. Fray, J.E. Molloy, M.O. Armitage, and J.C. Sparrow. Quantification of single human dermal fibroblast contraction. *Tissue Engineering*, 4:281–291, 1998.
- J. Genzer and J. Groenewold. Soft matter with hard skin: From skin wrinkles to templating and material characterization. *Soft Matter*, 2:310–323, 2006.
- K. Ghosh, Z. Pan, E. Guan, S. Ge, Y. Liu, T. Nakamura, Z.-D. Ren, M. Rafailovich, and R.A.F. Clark. Cell adaptation to a physiologically relevant ECM mimic with different viscoelastic properties. *Biomaterials*, 28:671–679, 2007.
- F. Grinnell. Mini-review on the cellular mechanisms of disease - fibroblasts, myofibroblasts, and wound contraction. *The Journal of Cell Biology*, 124:401–404, 1994.
- F. Grinnell. Fibroblast-collagen-matrix contraction: growth-factor signalling and mechanical loading. *Trends in Cell Biology*, 10:362–365, 2000.
- F. Grinnell. Fibroblast biology in three-dimensional collagen matrices. *Trends in Cell Biology*, 13:264–269, 2003.
- C.L. Hall. *Modelling of some biological materials using continuum mechanics*. PhD thesis, Queensland University of Technology, 2009.

- J.M. Haugh. Deterministic model of dermal wound invasion incorporating receptor-mediated signal transduction and spatial gradient sensing. *Biophysical Journal*, 90:2297–2308, 2006.
- O.R. Herber, W. Schnepf, and M.A. Rieger. A systematic review on the impact of leg ulceration on patients’ quality of life. *Health and Quality of Life Outcomes*, 5:1–12, 2007.
- B. Hinz. Formation and function of the myofibroblast during tissue repair. *Journal of Investigative Dermatology*, 127:526–537, 2007.
- B. Hinz. The myofibroblast: Paradigm for a mechanically active cell. *Journal of Biomechanics*, 43:146–155, 2010.
- B. Hinz, D. Mastrangelo, C.E. Iselin, C. Chaponnier, and G. Gabbiani. Mechanical tension controls granulation tissue contractile activity and myofibroblast differentiation. *American Journal of Pathology*, 159:1009–1020, 2001.
- E. Javierre, P. Moreo, M. Doblare, and J.M. Garcia-Aznar. Numerical modeling of a mechano-chemical theory for wound contraction analysis. *International Journal of Solids and Structures*, 46:3597–3606, 2009.
- G. Jenkins. The role of proteases in transforming growth factor- β activation. *The International Journal of Biochemistry and Cell Biology*, 40:1068–1078, 2008.
- D.F. Kennedy and W.J. Cliff. A systematic study of wound contraction in mammalian skin. *Pathology*, 11:207–222, 1979.
- Y. Kim and A. Friedman. Interaction of tumor with its micro-environment: A mathematical model. *Bulletin of Mathematical Biology*, 2009. Published online.
- S.K. Masur, H.S. Dewal, T.T. Dinh, I. Erenburg, and S. Petridou. Myofibroblasts differentiate from fibroblasts when plated at low density. *Proceedings of the National Academy of Science of the United States of America*, 93:4219–4223, 1996.
- S. McDougall, J.C. Dallon, J.A. Sherratt, and P.K. Maini. Fibroblast migration and collagen deposition during dermal wound healing: mathematical modelling and clinical implications. *Philosophical Transactions of the Royal Society A*, 364:1385–1405, 2006.
- M.H. McGrath and R.H. Simon. Wound geometry and the kinetics of wound contraction. *Plastic and Reconstructive Surgery*, 72:66–72, 1983.
- S.N. Menon, J.A. Flegg, S.W. McCue, R.C. Schugart, R.A. Dawson, and D.L.S. McElwain. Modelling the interaction of keratinocytes and fibroblasts during the wound healing process. *Submitted*, -:1–8, 2011.

- D.M. Monroe, N. Mackman, and M. Hoffman. Wound healing in hemophilia B mice and low tissue factor mice. *Thrombosis Research*, 125:S74–S77, 2010.
- V. Moulin, G. Castilloux, A. Jean, D.R. Garrel, F.A. Auger, and L. Germain. In vitro models to study wound healing fibroblasts. *Burns*, 22:359–362, 1996.
- V. Moulin, G. Castilloux, F.A. Auger, D.R. Garrel, M.D. O’Connor-McCourt, and L. Germain. Modulated response to cytokines of human wound healing myofibroblasts compared to dermal fibroblasts. *Experimental Cell Research*, 238: 283–293, 1998.
- V. Moulin, S. Larochelle, C. Langlois, I. Thibault, C.A. Lopez-Vallé, and M. Roy. Normal skin wound and hypertrophic scar myofibroblasts have differential responses to apoptotic inductors. *Journal of Cellular Physiology*, 198:350–358, 2004.
- K.E. Murphy, C.L. Hall, S.W. McCue, and D.L.S. McElwain. A two-compartment mechanochemical model of the roles of transforming growth factor β and tissue tension in dermal wound healing. *Journal of Theoretical Biology*, 272:145–159, 2011.
- J.D. Murray. *Mathematical Biology II: Spatial Models and Biomedical Applications*, volume 18 of *Interdisciplinary Applied Mathematics*. Springer, 3 edition, 2003.
- J.D. Murray, P.K. Maini, and R.T. Tranquillo. Mechanochemical models for generating biological pattern and form in development. *Physics Reports*, 2:59–84, 1988.
- J.D. Murray, J. Cook, R. Tyson, and S.R. Lubkin. Spatial pattern formation in biology: I. dermal wound healing. ii. bacterial patterns. *Journal of the Franklin Institute*, 335:303–332, 1997.
- L. Olsen, J.A. Sherratt, and P.K. Maini. A mechanochemical model for adult dermal wound contraction and the permanence of the contracted tissue displacement profile. *Journal of Theoretical Biology*, 17:113–128, 1995.
- L. Olsen, J.A. Sherratt, and P.K. Maini. A mathematical model for fibroproliferative wound healing disorders. *Bulletin of Mathematical Biology*, 58: 787–808, 1996.
- L. Olsen, J.A. Sherratt, and P.K. Maini. A mechanochemical model for normal and abnormal dermal wound repair. *Nonlinear Analysis*, 30:3333–3338, 1997.
- L. Olsen, J.A. Sherratt, and P.K. Maini. Spatially varying equilibria of mechanical models: Application to dermal wound contraction. *Mathematical Biosciences*, 147:113–129, 1998.

- L. Olsen, P.K. Maini, J.A. Sherratt, and J.C. Dallon. Mathematical modelling of anisotropy in fibrous connective tissue. *Mathematical Biosciences*, 158:145–170, 1999.
- C. Overall, J. Wrana, and J. Sodek. Transcriptional and post-transcriptional regulation of 72-kDa gelatinase/type IV collagenase by transforming growth factor- β 1 in human fibroblasts. *The Journal of Biological Chemistry*, 266:14064–14071, 1991.
- G. Pettet, M.A.J. Chaplain, D.L.S. McElwain, and H.M. Byrne. On the role of angiogenesis in wound healing. *Proceedings of the Royal Society: Biological Sciences*, 263:1487–1493, 1996.
- S. Ramtani. Mechanical modelling of cell/ECM and cell/cell interactions during the contraction of a fibroblast-populated collagen microsphere: theory and model simulation. *Journal of Biomechanics*, 37:1709–1718, 2004.
- S. Ramtani, E. Fernandes-Morin, and D. Geiger. Remodeled-matrix contraction by fibroblasts: numerical investigations. *Computers in Biology and Medicine*, 32:283–296, 2002.
- A.B. Roberts, K.C. Flanders, U.E. Heine, S. Jakowlew, P. Knodaiah, S.-J Kim, and M.B. Sporn. Transforming growth factor- β : Multifunctional regulator of differentiation and development. *Philosophical Transactions of the Royal Society of London. Series B, Biological Sciences*, 327:145–154, 1990.
- R.C. Schugart, A. Friedman, R. Zhao, and K.S. Chandan. Wound angiogenesis as a function of tissue tension: A mathematical model. *Proceedings of the National Academy of Sciences of the United States of America*, 105:2628–2633, 2008.
- G.S. Shultz, G. Ladwig, and A. Wysocki. Extracellular matrix: review of its roles in acute and chronic wounds. Published online at World Wide Wounds, URL: <http://www.worldwidewounds.com/2005/august/Schultz/Extrace-Matric-Acute-Chronic-Wounds.html>, 2005.
- A.L. Sillman, D.M. Quang, B. Farboud, K.S. Fang, R. Nuccitelli, and R.R. Isseroff. Human dermal fibroblasts do not exhibit directional migration on collagen 1 in direct-current electric fields of physiological strength. *Experimental Dermatology*, 12:396–402, 2003.
- F.H. Silver, J.W. Freeman, and D. DeVore. Viscoelastic properties of human skin and processed dermis. *Skin Research and Technology*, 7:18–23, 2001.
- A.J. Singer and R.A.F. Clark. Cutaneous wound healing. *The New England Journal of Medicine*, 341:738–747, 1999.

- R. Skalak, S. Zargaryan, R.K. Jain, P.A. Netti, and A. Hoger. Compatibility and the genesis of residual stress by volumetric growth. *Journal of Mathematical Biology*, 34:889–914, 1996.
- F. Strutz, M. Zeisberg, A. Renziehausen, B. Raschke, V. Becker, C. van Kooten, and G. Muller. TGF- β 1 induces proliferation in human renal fibroblasts via induction of basic fibroblast growth factor (FGF-2). *Kidney International*, 59: 579–592, 2001.
- J.A. Thackham, D.L.S. McElwain, and R.J. Long. The use of hyperbaric oxygen therapy to treat chronic wounds: A review. *Wound Repair and Regeneration*, 16:321–330, 2008.
- R.G. Thorne, S. Hrabetova, and C. Nicholson. Diffusion of epidermal growth factor in rat brain extracellular space measured by integrative optical imaging. *Journal of Neurophysiology*, 92:3471–3481, 2004.
- J.J. Tomasek, G. Gabbiani, B. Hinz, C. Chaponnier, and R.A. Brown. Myofibroblasts and mechano-regulation of connective tissue remodelling. *Nature Reviews Molecular Cell Biology*, 3:349–363, 2002.
- P. Tracqui, D.E. Woodward, G.C. Cruywagen, J. Cook, and J.D. Murray. A mechanical model for fibroblast-driven wound healing. *Journal of Biological Systems*, 3:1075–1084, 1995.
- L. Tranqui and P. Tracqui. Mechanical signalling and angiogenesis. the integration of cell-extracellular matrix couplings. *Life Sciences*, 323:31–47, 2000.
- R.T. Tranquillo and J.D. Murray. Continuum model of fibroblast-driven wound contraction: Inflammation-mediation. *Journal of Theoretical Biology*, 158:135–172, 1992.
- J.S. Vande Berg, R. Rudolph, W.L. Poolman, and D.R. Disharoon. Comparative growth dynamics and active concentration between cultured human myofibroblasts from granulating wounds and dermal fibroblasts from normal skin. *Laboratory Investigation*, 61:532–538, 1989.
- F.J. Vermolen and E. Javierre. Computer simulations from a finite-element model for wound contraction and closure. 19:43–53, 2010.
- R. Wang, A. Ghahary, Q. Shen, P.G. Scott, K. Roy, and E.E. Tredget. Hypertrophic scar tissues and fibroblasts produce more transforming growth factor- β 1 mRNA and protein than normal skin and cells. *Wound Repair and Regeneration*, 8: 128–137, 2000.

- G.T. Watts. Wound shape and tissue tension in healing. *The British Journal of Surgery*, 47:555–561, 1960.
- H.V. Waugh and J.A. Sherratt. Macrophage dynamics in diabetic wound healing. *Bulletin of Mathematical Biology*, 68:197–207, 2006.
- R.G. Wells and D.E. Discher. Matrix elasticity, cytoskeletal tension, and TGF β : The insoluble and soluble meet. *Science Signaling*, 1:pe13, 2008.
- P.-J. Wipff and B. Hinz. Integrins and the activation of latent transforming growth factor β 1 - an intimate relationship. *Journal of Cell Biology*, 87:601–615, 2008.
- P.-J. Wipff and B. Hinz. Myofibroblasts work best under stress. *Journal of Bodywork and Movement Therapies*, 13:121–127, 2009.
- P.-J. Wipff, D.B. Rifkin, J.-J. Meister, and B. Hinz. Myofibroblast contraction activates latent TGF- β 1 from the extracellular matrix. *Journal of Cell Biology*, 179:1311–1323, 2007.
- L.K. Wrobel, T.R. Fray, J.E. Molloy, J.J. Adams, M.P. Armitage, and J.C. Sparrow. Contractility of single human dermal myofibroblasts and fibroblasts. *Cell Motility and the Cytoskeleton*, 52:82–90, 2002.
- C. Xue, A. Friedman, and C.K. Sen. A mathematical model of ischemic cutaneous wounds. *Proceedings of the National Academy of Sciences*, 106:16782–16787, 2009.
- L. Yang, C.X. Qiu, A. Ludlow, M.W.J. Ferguson, and G. Brunner. Active transforming growth factor- β in wound repair: Determination using a new assay. *American Journal of Pathology*, 154:105–111, 1999.

Appendix A. Non-Dimensional Equations

Applying the following non-dimensionalization

$$\begin{aligned}
\hat{N} &= \frac{r}{\theta_{nn}}, & \hat{B} &= \beta_0, & \hat{Z}^2 &= \frac{a_z k \hat{N}^2}{\delta_\rho \delta_\zeta}, & \hat{R} &= \frac{k \hat{N}}{\delta_\rho \hat{Z}}, & \hat{V} &= \frac{L}{T} \\
\bar{D}_n &= \frac{D_n T}{L^2}, & \bar{\alpha} &= \alpha B T, & \bar{a}_{n\beta} &= a_{n\beta} \hat{B}, & \bar{a}_n &= r T, & \bar{a}_{m\sigma} &= a_{m\sigma} T, \\
\bar{a}_{m\beta} &= a_{m\beta} \hat{B}, & \bar{\theta}_m &= \theta_m T, & \bar{\theta}_{mm} &= \theta_{mm} \hat{N} T, & \bar{a}_\beta &= a_\beta \hat{N} T, & \bar{b}_\beta &= b_\beta \hat{B}, \\
\bar{D}_\beta &= \frac{D_\beta T}{L^2}, & \bar{\eta} &= \eta, & \bar{a}_{\beta m} &= \frac{a_{\beta m} \hat{N} \hat{R} T}{\hat{B}}, & \bar{a}_{\beta z} &= a_{\beta z} \hat{Z} T, & \bar{\delta}_\beta &= \delta_\beta T, \\
\bar{K} &= \frac{k \hat{N} T}{\hat{R}}, & \bar{a}_{\rho\beta} &= a_{\rho\beta} \hat{B}, & \bar{\omega} &= \delta_\zeta T, & \bar{b}_\zeta &= b_\zeta \hat{B}, & \bar{s} &= s L^2, \\
\bar{E} &= E, & \bar{\mu} &= \frac{\mu}{\hat{R} T}, & \bar{\lambda} &= \lambda \hat{N}, & \bar{\xi} &= \xi, & \bar{\pi} &= \pi, \\
\bar{\zeta} &= \zeta, & \hat{P} &= P_0, & \bar{\chi} &= \frac{\chi T}{L^2 \hat{P}}, & \bar{a}_\chi &= \frac{a_\chi}{\hat{P}}, & \bar{D}_P &= \frac{D_P T}{L^2}, \\
\bar{a}_P &= \frac{a_P T}{\hat{P}}, & \bar{\delta}_P &= \delta_P T, & \bar{\delta}_{Pn} &= \delta_{Pn} T \hat{N},
\end{aligned}$$

and dropping bars, we obtain the following non-dimensional equations,

$$\begin{aligned}
\frac{\partial n}{\partial t} + \frac{\partial}{\partial x} (nv) &= \frac{\partial}{\partial x} \left[D_n \frac{\partial n}{\partial x} - \frac{\chi n}{(a_\chi + P)^2 \frac{\partial P}{\partial x}} \right] \\
&\quad + r(1 + a_{n\beta}\beta)n(1 - n) - \alpha\sigma^+\beta n, \tag{A.1}
\end{aligned}$$

$$\frac{\partial m}{\partial t} + \frac{\partial}{\partial x} (mv) = m(a_{m\sigma}\sigma^+(1 + a_{m\beta}\beta) - \theta_m - \theta_{mm}m) + \alpha\sigma^+\beta n, \tag{A.2}$$

$$\frac{\partial \beta}{\partial t} + \frac{\partial}{\partial x} (\beta v) = D_\beta \frac{\partial^2 \beta}{\partial x^2} + \frac{a_\beta \beta (n + \pi m)}{1 + b_\beta \beta} + a_{\beta m} m \rho + a_{\beta z} z \beta - \delta_\beta \beta \tag{A.3}$$

$$\frac{\partial P}{\partial t} + \frac{\partial}{\partial x} (Pv) = D_P \frac{\partial^2 P}{\partial x^2} + a_P - \delta_P P - \delta_{Pn} n P, \tag{A.4}$$

$$\frac{\partial \rho}{\partial t} + \frac{\partial}{\partial x} (\rho v) = \kappa((n + \eta m)(1 + a_{\rho\beta}\beta) - \rho z), \tag{A.5}$$

$$\frac{\partial z}{\partial t} + \frac{\partial}{\partial x} (zv) = \omega \left(\frac{\rho(n + \zeta m)}{1 + b_z \beta} - z \right), \tag{A.6}$$

$$s\rho u = \frac{\partial}{\partial x} \left(\sigma + \mu \frac{\partial v}{\partial x} + \psi \right), \tag{A.7}$$

$$\sigma = E\rho \frac{\partial u}{\partial x}, \tag{A.8}$$

$$\psi = \lambda\rho(n + \xi m), \tag{A.9}$$

$$v = \frac{\partial u}{\partial t}. \tag{A.10}$$

Appendix B. Initial Conditions

The following represent the scaled initial conditions employed in this model

$$n(x, 0) = \frac{1}{2} \left\{ 1 + \tan \left(\frac{x - L}{\epsilon_n} \right) \right\}, \quad (\text{B.1})$$

$$m(x, 0) = 0, \quad (\text{B.2})$$

$$\beta(x, 0) = \frac{1}{2} \left\{ 1 - \tan \left(\frac{x - L}{\epsilon_\beta} \right) \right\}, \quad (\text{B.3})$$

$$P(x, 0) = \frac{1}{2} \left\{ (P_{ss} + P_{in}) + (P_{ss} - P_{in}) \tan \left(\frac{x - L}{\epsilon_\rho} \right) \right\}, \quad (\text{B.4})$$

$$\rho(x, 0) = \frac{1}{2} \left\{ (1 + \rho_{in}) + (1 - \rho_{in}) \tan \left(\frac{x - L}{\epsilon_\rho} \right) \right\}, \quad (\text{B.5})$$

$$z(x, 0) = \frac{1}{2} \left\{ 1 + \tan \left(\frac{x - L}{\epsilon_z} \right) \right\}, \quad (\text{B.6})$$

where $\epsilon_n = 0.1$, $\epsilon_\beta = \epsilon_\rho = \epsilon_z = 0.4$, controlling the steepness across the boundary, $\rho_{in} = 0.1$, the initial scaled collagen density within the wound space, P_{ss} is the steady-state value for PDGF in the presence of fibroblasts, given by $P_{ss} = a_P / (\delta_P + \delta_{Pn}n)$, $P_{in} = a_P / \delta_P$, is the steady-state value for PDGF in the absence of fibroblasts and $L = 1$, the scaled initial position of the wound boundary.

Appendix C. Parameter Estimation

First, we estimate values for the scalings used to non-dimensionalize the variables:

L : A typical length scale for acute dermal wounds is 1cm.

T : A typical length scale for time is days. Hence, $T = 1$ day.

r : In Murphy et al. (2011) we estimate fibroblast proliferation to be $r = 0.832/\text{day}$.

θ_{nn}^{-1} : The carrying capacity of fibroblasts is known to be approximately $10^6/\text{mL}$ (Vande Berg et al., 1989). Hence, we take $\theta_{nn}^{-1} = 10^6 \text{cells/mL}$.

k/δ_ρ : It is known that 30% of newly synthesized collagen is degraded (Aumailley et al., 1982). Hence, $\delta_\rho = 0.3k$, such that $k/\delta_\rho = 3.33$. Bahar et al. (2004) estimates a collagen production rate of 1.75pg/cell.day .

β_0 : Yang et al. (1999) found the initial concentration of $\text{TGF}\beta$ in the wound to be 275ng/mL . Hence, we take $\beta_0 = 275 \text{ng/mL}$.

P_0 : Menon et al. (2011) estimate the steady-state density of PDGF to be $47.8\text{ng}/\text{cm}^3$.

We can now apply the following non-dimensionalization.

$$\begin{aligned}\bar{x} &= \frac{x}{L}, & \bar{t} &= \frac{t}{T}, & \bar{n} &= \frac{n}{\hat{N}}, & \bar{m} &= \frac{m}{\hat{N}}, & \bar{P} &= \frac{P}{P_0}, \\ \bar{\rho} &= \frac{\rho}{\hat{R}}, & \bar{z} &= \frac{z}{\hat{Z}}, & \hat{\beta} &= \frac{\beta}{\beta_0}, & \bar{u} &= \frac{u}{L}, & \bar{v} &= \frac{Tv}{L},\end{aligned}$$

The values for the remaining dimensional parameters are as follows.

D_n : Experiments by Sillman et al. (2003) found that fibroblasts derived from normal human dermal wounds migrate at an average velocity of $0.23 - 0.36\mu\text{m}/\text{min}$. This gives a range for the minimum wavespeed of $0.00033 < D_n < 0.001\text{cm}^2/\text{day}$. We choose the upper limit of $D_n = 0.001\text{cm}^2/\text{day}$.

χ : We use the value proposed by Haugh (2006) and Menon et al. (2011) of $\chi = 4.78 \times 10^{-3}\text{ng}/\text{cm}\cdot\text{day}$.

a_χ : Re-dimensionalizing the parameters given by Menon et al. (2011), the half-maximal response occurs when $a_\chi = 47.8\text{ng}/\text{cm}^3$.

$a_{n\beta}$: Strutz et al. (2001) found $\text{TGF}\beta$ to increase fibroblast proliferation by 2 – 3 times. Hence, we assume that $a_{n\beta} = 2/\beta_0$.

α : Desmouliere et al. (1993) found that culturing fibroblasts in the presence of $\text{TGF}\beta$ increased the percentage of cells expressing $\alpha\text{-SMA}$ from 7.5% to 45.3%, representing an activation of 37.8% of fibroblasts, and is consistent with other estimates (Masur et al., 1996; Moulin et al., 1996). This experiment occurred over a one week period, with a $\text{TGF}\beta$ dose of $5 - 10\text{ng}/\text{mL}$. This gives a range for the activation of $0.0054 < \alpha < 0.0108/\text{day}\cdot(\text{ng}/\text{mL})$. We choose the upper limit of $\alpha = 0.0108/\text{day}\cdot(\text{ng}/\text{mL})$.

$a_{m\sigma}$: We assume that myofibroblasts proliferate slowly under stress, with a rate proportional to the fibroblast proliferation rate, such that $a_{m\sigma} = 0.25r$.

$a_{m\beta}$: We assume that myofibroblasts experience the same increase in proliferation due to $\text{TGF}\beta$ as fibroblasts. Hence, $a_{m\beta} = a_{n\beta}$.

θ_m : The doubling time of fibroblasts is approximately 18 hours (Olsen et al., 1995). We assume that the doubling time of myofibroblasts is the same as that for fibroblasts. Hence, this gives a natural cell death rate for the myofibroblasts of $\theta_m \approx 0.90$.

θ_{mm} : As myofibroblasts are roughly twice the size of fibroblasts (Masur et al.,

1996), we assume that myofibroblasts have half the carrying capacity of fibroblasts, i.e., $\theta_{mm} = 2\theta_{nn} = (0.5 \times 10^6)^{-1}$.

D_β : Using known estimates of the molecular weight of epidermal growth factor (EGF) and TGF β (Cell Signaling Technology, 2010) and the diffusivity of epidermal growth factor (Thorne et al., 2004), we were able to determine the diffusivity of TGF β using the Stokes-Einstein formula, such that $D_\beta \approx 0.0254\text{cm}^2/\text{day}$.

a_β : Experiments by Wang et al. (2000) give the range for TGF β production by fibroblasts as $0.125 < a_\beta < 0.525 \times 10^{-6}\text{ng}/(\text{cell}\cdot\text{day})$. We choose the lower limit, such that $a_\beta = 0.125 \times 10^{-6}\text{ng}/(\text{cell}\cdot\text{day})$.

η : On a percentage basis, myofibroblasts produce roughly twice the collagen that is synthesized by fibroblasts (Kim and Friedman, 2009; Moulin et al., 1998; Olsen et al., 1995). Hence, we choose $\eta = 2$. We assume a similar trend for myofibroblast synthesis of TGF β and collagenase. Hence, $\pi = \zeta = \eta = 2$.

b_β : Using estimates from Dale (1995), inhibition of TGF β synthesis is assumed to be $b_\beta = 0.0013\text{mL}/\text{ng}$.

$a_{\beta z}$: Using order of magnitude approximation, we estimate the activation of TGF β by collagenase as $0.00144\text{ng}/\text{cell}$.

$a_{\beta m}$: We assume that the amount of TGF β activated from matrix stores is of the same order of magnitude as the amount of TGF β activated by collagenase following non-dimensionalization. Hence, we estimate the activation of TGF β by myofibroblasts to be $4.35 \times 10^{-9}\text{mL}\cdot\text{day}/\text{cell}$.

δ_β : The TGF β decay rate was estimated from the exponential phase of the data from Yang et al. (1999), giving a rate of $\delta_\beta \approx 0.354/\text{day}$.

D_P : Schugart et al. (2008) gives the range for PDGF diffusion as $7.44 \times 10^{-4} < D_P < 1.416 \times 10^{-2}\text{cm}^2/\text{day}$, while both Haugh (2006) and Menon et al. (2011) take the value $D_P = 2.4 \times 10^{-3}\text{cm}^2/\text{day}$, which we note is within the interval proposed by Schugart et al. (2008). Hence, we take $D_P = 2.4 \times 10^{-3}\text{cm}^2/\text{day}$.

a_P : Menon et al. (2011) choose the value of a_P so that it balances the natural decay term in the absence of fibroblasts. Applying the same logic, this yields a value for PDGF production of $a_P = 115\text{ng}/\text{cm}^3\cdot\text{day}$.

δ_P : Olsen et al. (1995), Haugh (2006) and Menon et al. (2011) all consider PDGF decay to be $O(1)/\text{day}$. We use the value given by Haugh (2006) of $\delta_P = 2.4/\text{day}$.

δ_{Pn} : Haugh (2006) estimate the range for the fibroblast consumption of PDGF to be $2.4 < \delta_{Pn} < 48/\text{day}$. Following Menon et al. (2011), we take the upper limit, and taking account of the number of cells, take $\delta_{Pn} = 4.8 \times 10^{-5}/\text{cell.day}$.

$a_{\rho\beta}$: Eickelberg et al. (1999) found a 2 – 3-fold increase in collagen expression by human lung fibroblasts in the presence of TGF β . We assume that TGF β induces a similar increase in collagen production by dermal fibroblasts. Hence, we estimate that $a_{\rho\beta} = 2/\beta_0$.

a_z : We assume that the non-dimensional collagen growth parameter, κ , should be of $O(10^{-1})$. This gives an estimate of $a_z = 4.73 \times 10^{-9} (\text{ng/mL})^{-2}.\text{day}$.

b_z : Overall et al. (1991) found a reduction of 66 – 75% of collagenase synthesis in the presence of TGF β . This gives an estimate of $b_z = 3/\beta_0$.

δ_z : Overall et al. (1991) estimate the half-life of MMP-2 as 46 hours. We assume that collagenase (MMP-1) has the same half-life, giving a decay rate of 0.3616/day.

s : Following Tranquillo and Murray (1992), Olsen et al. (1995) and Javierre et al. (2009), we consider a tethering coefficient of $s = 1$.

μ : We follow Olsen et al. (1995) and Javierre et al. (2009), and choose μ such that its non-dimensional value is 20.

E : Estimates of E range from 1 – 300N/cm² (Silver et al., 2001; Genzer and Groenewold, 2006). We consider an area of approximately 1cm², which gives a range of E of $10 < E < 300\text{N}$. We use the lower limit, such that $E = 10\text{N}$.

τ : In Murphy et al. (2011), we estimated a range for τ of $1 < \tau < 3\mu\text{N}/\text{cell}$. Hence, we consider a value of $\tau = 2.65\mu\text{N}/\text{cell}$, consistent with Fray et al. (1998) and Wrobel et al. (2002).

ζ : Wrobel et al. (2002) found that myofibroblasts can apply up to twice the cell traction force generated by fibroblasts. Hence, we choose $\xi = 2$.

RECENT REPORTS

22/11	A novel model for one-dimensional morphoelasticity. Part II: Application to the contraction of fibroblast-populated collagen lattices	Hall Menon McCue McElwain
23/11	Positive or negative Poynting effect? The role of adscititious inequalities in hyperelastic materials	Mihai Goriely McCue McElwain
24/11	On approaches to modelling lattice dislocations	Hall Markenscoff
25/11	Nonlinear waves in heterogeneous elastic rods via homogenization	de Luna Emptage Goriely Bressloff
26/11	Synaptic bistability due to nucleation and evaporation of receptor clusters	Burlakov Duričković Goriely
27/11	Particle trapping and banding in rapid solidification	Elliot Peppin
28/11	Growth of confined cancer spheroids: a combined experimental and mathematical modelling approach	Loessner Flegg Byrne Hall Moroney Clements McElwain Hutmacher
29/11	Floating carpets and the delamination of elastic sheets	Wagner Vella
30/11	Numerical Study of Liquid Crystal Elastomers by a Mixed Finite	Luo Calderer
31/11	The indentation of pressurized elastic shells: From polymeric capsules to yeast cells	Vella Ajdari Vaziri Boudaoud
32/11	Wrinkling of pressurized elastic shells	Vella Ajdari Vaziri Boudaoud
33/11	Data assimilation using bayesian filters and B-spline geological models	Duan Farmer Hoteit Lu Moroz
34/11	Review of nonlinear Kalman, ensemble and particle filtering with application to the reservoir history matching problem	Luo Hoteit Duan

37/11	Frequency jumps in the planar vibrations of an elastic beam	Neukirch Frelat Goriely Maurini
38/11	Ice-lens formation and con nemenent-induced supercooling in soils and other colloidal materials	Style Cocks Peppin Wettlaufer
39/11	An asymptotic theory for the re-equilibration of a micellar surfac- tant solution	Griffiths Bain Breward Chapman Howell Water
40/11	Higher-order numerical methods for stochastic simulation of chemical reaction systems	Székelly Burrage Erban Zygalakis
41/11	On the modelling and simulation of a high pressure shift freezing process	Smith Peppin Ángel M. Ramos
42/11	An efficient implementation of an implicit FEM scheme for fractional-in-space reaction-diffusion equations	Burrage Hale Kay
43/11	Coupling fluid and solute dynamics within the ocular surface tear film: a modelling study of black Line osmolarity	Zubkov Breward Gaffney
44/11	A prototypical model for tensional wrinkling in thin sheets	Davidovitch Schroll Vella Adda-Bedia Cerde

**Copies of these, and any other OCCAM reports can be obtained
from:**

**Oxford Centre for Collaborative Applied Mathematics
Mathematical Institute
24 - 29 St Giles'
Oxford
OX1 3LB
England**

www.maths.ox.ac.uk/occam